Twin Spray Characteristics Between Two Impinging F-O-O-F Type Injectors

Shin-Jae Kang
Faculty of Mechanical and Aerospace System Engineering, Chonbuk National University, Chonbuk 561-756, Korea
Eun-Sang Lee, Ki-Chul Kwon, Je-Ha Oh
Graduate School, Chonbuk National University, Chonbuk 561-756, Korea
Myoung-Jong Yu
Post-Doc. Chonbuk National University, Chonbuk 561-756, Korea

This paper presents twin spray characteristics of two impinging F-O-O-F type injectors in which fuel and oxidizer impinge on each other to atomize under the various conditions. The droplet size and velocity in the impinging spray flow field were measured using PDPA. The droplet size and velocity were investigated at the mixture ratios of 1.5, 2.0, 2.47 and 3.0 for four injectors in which two single F-O-O-F injectors were arranged at the intervals of 20.8, 31.2, 41.6 and 62.4mm respectively. In general, the arithmetic mean diameter, SMD and standard deviation of droplet size in the interaction area (X=0 and Y=0mm) were smaller, while the axial velocity in the interaction area was slightly higher. An empirical correlation is obtained for the $(D_{10})_D/(D_{10})_C$ value under the assumptions of two identical droplets and these with different size and velocity. The droplets with low Weber numbers below 40 have possibility to coalesce, while those over 40 tend to disintegrate after impingement in the interaction area.

Key Words: Impinging Injector, Twin Spray, Interaction Area, Phase Doppler Particle Analyzer (PDPA)

Nomenclature

L : Interval length between injectors [mm]
r : Mixture ratio
$\dot{m}$: Mass flow rate [g/s]
D_{10} : Arithmetic mean diameter [μm]
D_{32} : Sauter mean diameter [μm]
D_{sdev} : Standard deviation of droplets [μm]
U : Axial velocity [m/s]
We : Weber number

Subscripts
o : Oxidizer
f : Fuel
D : Centerline of interaction area

* Corresponding Author,
E-mail : kangsj@moak.chonbuk.ac.kr
TEL : +82-63-270-2387; **FAX** : +82-63-270-2472
Faculty of Mechanical and Aerospace System Engineering, Chonbuk National University, The Research Institute of Industrial Technology, 664-14, Dukjin-dong, Dukjin-gu, Chonju, Chonbuk 561-756, Korea. (Manuscript **Received** October 15, 2001; **Revised** February 8, 2002)

1. Introduction

A liquid rocket engine, which is employed widely in the middle · low thrust rocket system, has been investigated to improve the performance over the past half century. Since a rocket is a propulsion system, the most effective factor on the rocket performance is combustion. To normalize and stabilize the combustion performance of a propulsion system, thermal and fluid dynamic movement in the combustion chamber should be analyzed and investigated. The most crucial element governing the combustion chamber is an injector. Therefore, many recent studies have been concentrated on the performance analysis of injectors.

A liquid propellant propulsion system makes

combustion by the mixture of liquid fuel and oxidizer. During combustion, the atomizing procedure by impingement of fuel and oxidizer significantly influences the overall performance of a propulsion system. Hence, it is necessary that the spray characteristics of an injector should be thoroughly investigated to estimate its performance.

There have been many studies on the injector for a liquid rocket. Kuyjendal (1970) studied the effect of injection velocity, orifice diameter and impinging angle on the drop size for an impinging doublet type injector. Rupe (1956) tried to find correlation between mixture efficiency and orifice diameter, injection velocity and impinging angle for the doublet type injector. Also, Kang et al. (2000 ; 2001) analyzed the atomization characteristics with respect to the momentum ratio for the double impinging F-O-O-F type injector. Park et al. (1996) investigated the effect of the pressure drop, impinging angle and ratio of the orifice length to diameter on the droplet size using PDPA system for an unlike-triplet injector.

In a real liquid rocket engine, the spray characteristics of each injector as well as those in the interaction area between injectors significantly affect the combustion efficiency. Although the nozzle is composed of a lot of such injectors, the concept of this interaction area has not been closely examined. This paper is focused on the spray characteristics in the interaction area between injectors to investigate the atomization process and to obtain more detailed information on droplet formation. The available data to design a high performance rocket nozzle are presented.

2. Experimental Apparatus

2.1 Test facilities

Test facilities to investigate the atomization characteristics in the interaction area are composed of a simulant propellant feeding system, which delivers propellant from the tank to the injector, an injector forming the impinging jet and a PDPA system measuring the velocity and size of droplets. Water, which has ρ=998.2kg/m^3 and σ=0.073N/m at 20℃ under the standard atmospheric pressure, was used as a simulant liquid.

The injectors in which two single F-O-O-F injectors were arranged at intervals of L were used in this study, as shown in Fig. 1(a). Fuel is injected through the orifices ① and ④ and oxidizer through the orifices ② and ③. The fuel stream through orifice ① initially impinges on the oxidizer stream from ② (③ impinges on ④). These initially impinged jets impinge again and then form the spray. These second impinged jets

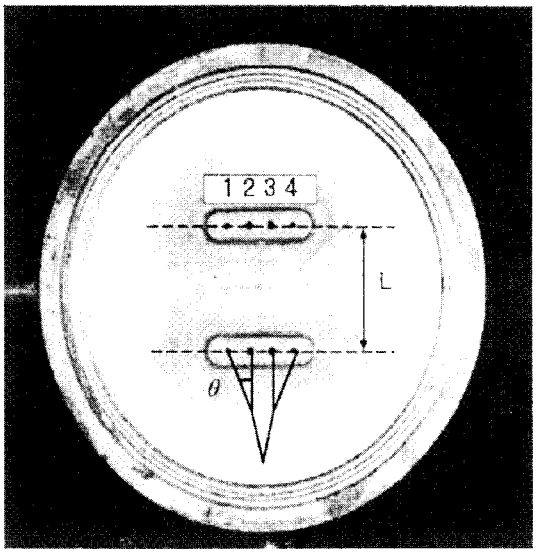

(a) Twin spray injector

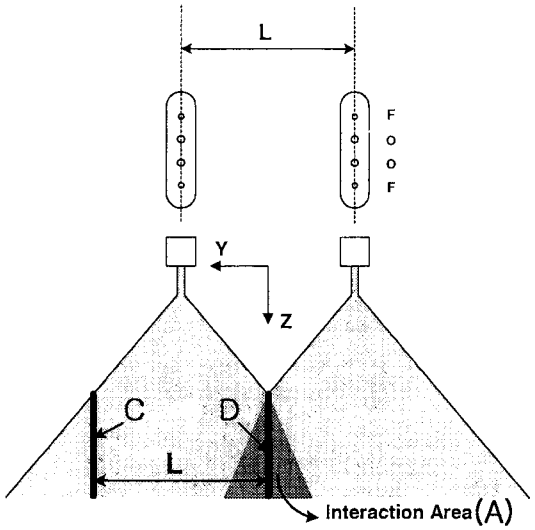

(b) Twin spray schematic

Fig. 1 Shape of injector

from two injectors meet in the A region, as shown in Fig. 1(b), since two injectors are closely located. Fuel orifices are located at an angle of $\theta=30$ with the central axis, and oxidizer orifices are parallel located. The diameter of fuel and oxidizer orifice is 1.6 and 22.mm respectively.

Figure 3 shows the schematic diagram of injection and PDPA system used in this study. An industrial displacement pump was employed to supply the propellant continuously to the injector at high pressure and flow rate. This pump can provide a maximum discharge flow rate of 99l/min and a maximum discharge pressure of 60kgf/cm^2. Three-dimensional phase Doppler particle analyzer (PDPA) was employed to measure atomized droplet size and velocity components. PDPA consists of an optical system, a signal processing system and a three-dimensional traversing system. The optical system is composed of transmitting & receiving optics, and a 350mW air-cooled Ar-ion laser was used. Transmitting optics make laser beam cross at the measurement point. Receiving optics detects the scattered light, which is produced when droplets pass through the measurement volume, and then transmit it to the signal processor. The signal processor (DANTEC model 58N50) is a burst detector type. Therefore, the size and velocity are measured by the frequency and relative phase difference of the Doppler signal. The voltage provided to the receiving optic sensor was fixed at 1400V. At each measuring point, 10000 of data sampling within 10 seconds were selected.

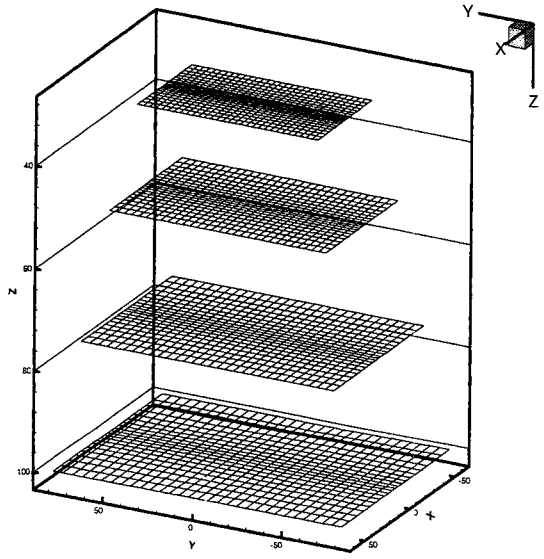

Fig. 2 Grid of measurement points

2.2 Experimental arrangement

The impinged jet formed by the injector has an elliptic structure. The flowing direction of the impinged jet, long-axis and short-axis direction

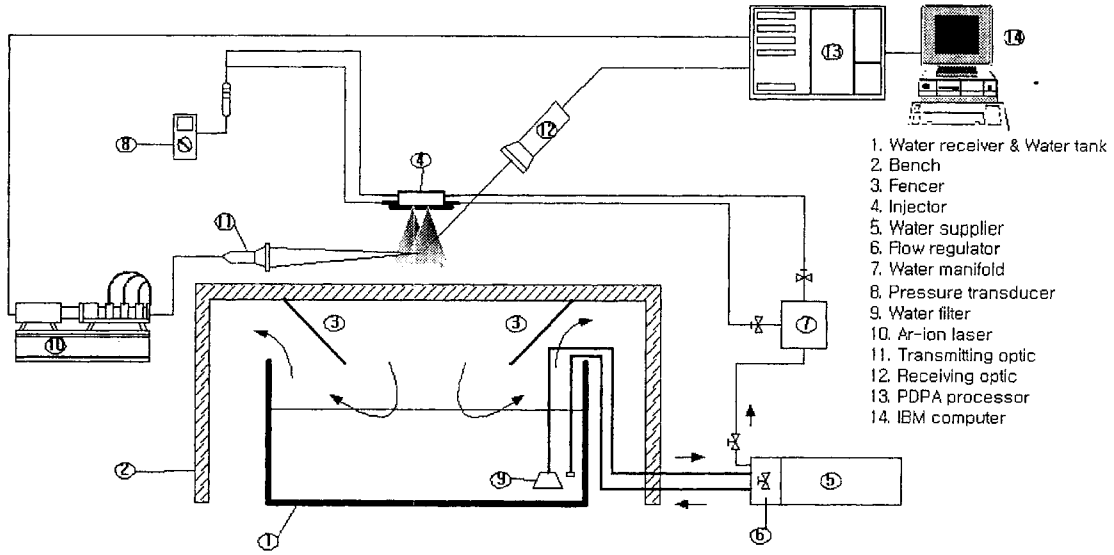

Fig. 3 Schematic diagram of injector and PDPA system

Table 1 Length between injectors

Injector	L(mm)
No. 1	20. 8
No. 2	31. 2
No. 3	41. 6
No. 4	62. 4

Table 2 Spray conditions

r	$\dot{m}_f$(g/s)	$\dot{m}_o$(g/s)
1.5	208.0	312.0
2.0	173.4	346.6
2.47	150.0	370.0
3.0	130.0	390.0

of ellipse are defined as Z, Y and X respectively. The velocity of Z-axis direction is defined as u.

The interval between two F-O-O-F type injectors, L, was varied to investigate twin spray characteristics in the interaction area in this study. The intervals (L) between injectors are indicated in Table 1.

The axial velocity and atomized droplet size were measured at various mixture ratios (r) defined as the dimensionless ratio of oxidizer flow rate to fuel flow rate, which a total flow rate was fixed at 520g/s. Table 2 shows the fuel and oxidizer flow rate for various mixture ratios used in this study.

$$mixture\ ratio(r)=\frac{oxidizer\ flow\ rate}{fuel\ flow\ rate}=\frac{\dot{m}_o}{\dot{m}_f} \quad (1)$$

For each mixture ratio, droplet size and velocity were measured in the cross sections parallel to the injector plane at the distances of 20mm, 30mm, 50mm and 100mm away from the injector plane. Each of cross sections has 651 measurement points, as shown in Fig. 2.

3. Results and Discussion

3.1 Droplet size

The arithmetic mean diameter (D_{10}) is generally used to investigate the atomization characteristics of the spray. The volume-surface mean diameter (D_{32}) is also used to analyze the behavior in the combustion chamber because the variation of the volume and surface area of the droplets is directly related to the chemical reactions including evaporation, heat transfer and combustion.

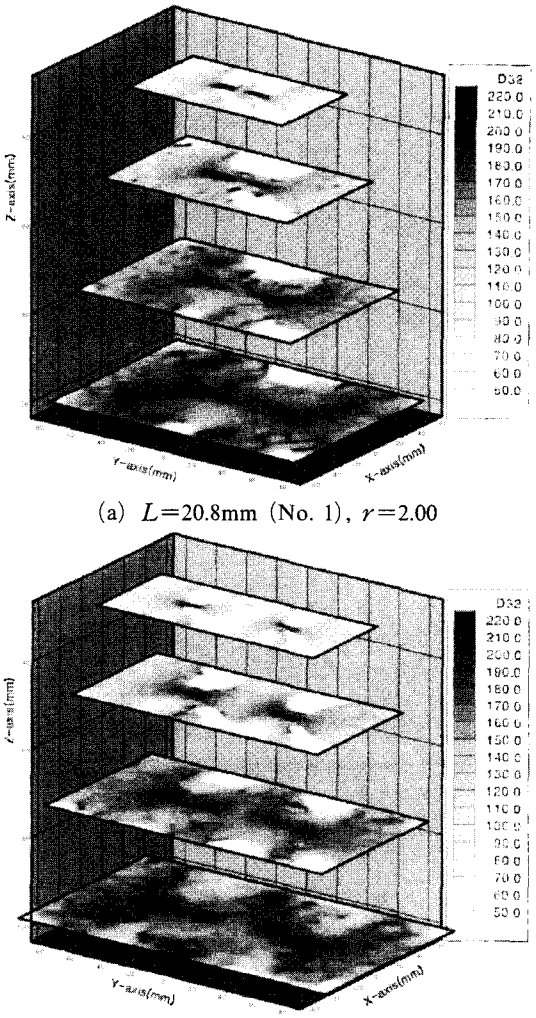

(a) L=20.8mm (No. 1), r=2.00

(b) L=62.4mm (No. 4), r=2.00

Fig. 4 SMD distribution

Figure 4 indicates the SMD distribution in the X-Y plane at r=2.0 for No. 1 and 6 injectors. There is an area where the data are not acquired in the cross section. This is because the high number density affects the acquisition. In case of the region near the injector plane, the SMD distribution is considerably high in the center of two single sprays because the second impinged jets are beginning to break into droplets irregularly and then coalesce each other. However, this trend disappears with moving into the down-

stream region, and droplets disintegrate into small. The SMD becomes small near Z=75mm. In the downstream region near Z=100mm, the momentum of jets decreases, so that droplets are not disintegrate any more but coalesce.

In Fig. 5 and 6, the SMD measured in the center, X=0mm, along the Y direction is non-dimensionalized with SMD_D at X=0mm and Y=0mm for No. 1 and 2 injectors. The position of Y/L=0 is the centerline of the interaction area of the twin spray, line D in Fig. 1(b), and Y/L=1 is C line. In case of both two injectors, since only few droplets superpose at Z=30mm, the SMD/SMD_D distribution between Y/L=0 and Y/L=1 is symmetric centering on Y/L=0.5. Also, the SMD/SMD_D value is high at the center of single spray, Y/L=0.5, since the arithmetic mean diameter of droplets disintegrated from liquid sheet is small but irregular (see Fig. 7 and 8). However, large size droplets are disintegrated into small by the impingement in the interaction area after Z=50mm, so that the drop size distribution becomes uniform. Hence, the SMD/SMD_D value in Y/L=1 exceeds 1 after Z=50mm. All four injectors have a similar tendency. This SMD distribution is very similar to the study of Yoon et al.(1992) on the interaction area for the pressure swirl nozzle.

The arithmetic mean diameter (D_{10}) measured in the center, X=0mm, along the Y direction is non-dimensionalized with the $(D_{10})_D$ at X=0mm and Y=0mm for No. 1 and 3 injectors in Fig. 7 and 8. In case of Z=30mm for No. 1 injector, the $D_{10}/(D_{10})_D$ value in Y/L=1 exceeds 1 at r=1.50 and 2.00, but it is smaller than 1 at r=2.47 and 3.00. It is considered that the

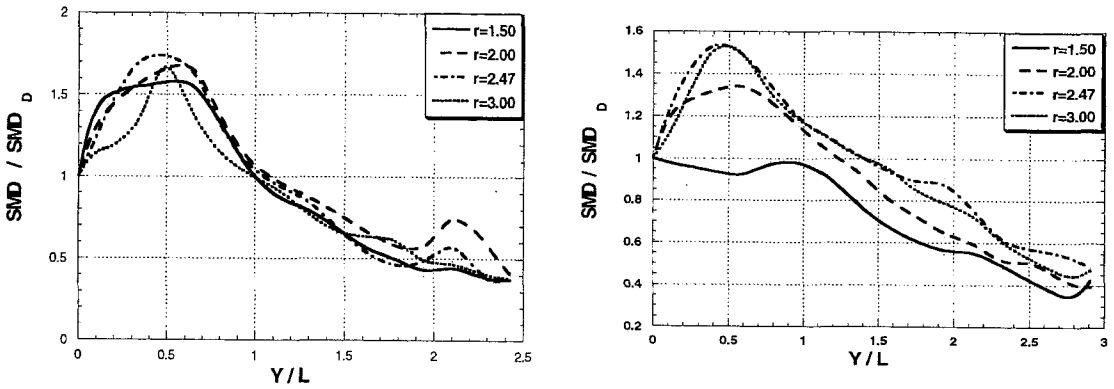

(a) Z=30mm (b) Z=50mm

Fig. 5 SMD/SMD_D distribution along the centerline (X=0mm) for No. 1 injector

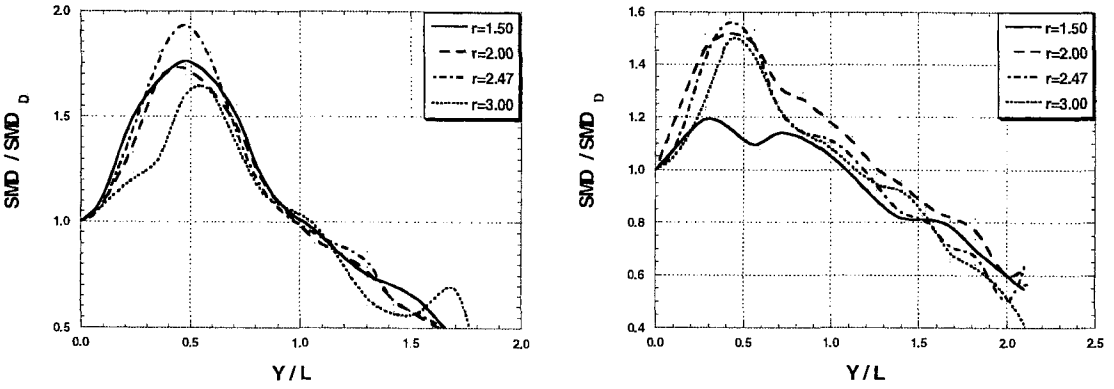

(a) Z=30mm (b) Z=50mm

Fig. 6 SMD/SMD_D distribution along the centerline (X=0mm) for No. 2 injector

position of $Y/L=1$ at $r=2.47$ and 3.00 is the outer region of the spray and relatively small droplets exist there, since the width of single spray becomes narrower with increasing the mixture ratio. Consequently, strong superposition of sprays do not occurred and the $D_{10}/(D_{10})_D$ value decreases with the mixture ratio at $Z=30$mm for No. 1 injector. The $D_{10}/(D_{10})_D$ value near $Y/L=0.5$ is smaller than in $Y/L=0$ and $Y/L=1$. This is considered that disintegration from liquid sheet into droplets is in process or just finished in the center of the single spray, $Y/L=0.5$. The $D_{10}/(D_{10})_D$ becomes uniform with moving into the downstream region. This is because small droplets become larger due to the coalescence and large droplets become smaller due to the disintegration, as droplets impinge each other in the interaction area. Also, the droplet size in the outer region of the spray increases with moving into the downstream region, since droplets coalesce each other due to the low momentum of droplets existed in the outer region. As shown in Fig. 8, the $D_{10}/(D_{10})_D$ distribution between $Y/L=0$ and $Y/L=1$ is symmetric centering on $Y/L=0.5$ at $Z=50$mm because there is no strong superposition of sprays. At $Z=75$ and 100mm, the superposition between two single sprays is occurred, and the distribution trend becomes similar to that for the No. 1 injector.

The uniformity, which means the distributed range of the droplet size physically, is directly related to the standard deviation of the droplet size in point of statistics. The standard deviation (D_{sdev}) of droplet size measured in the center, $X=0$mm, along the Y direction is non-dimen-

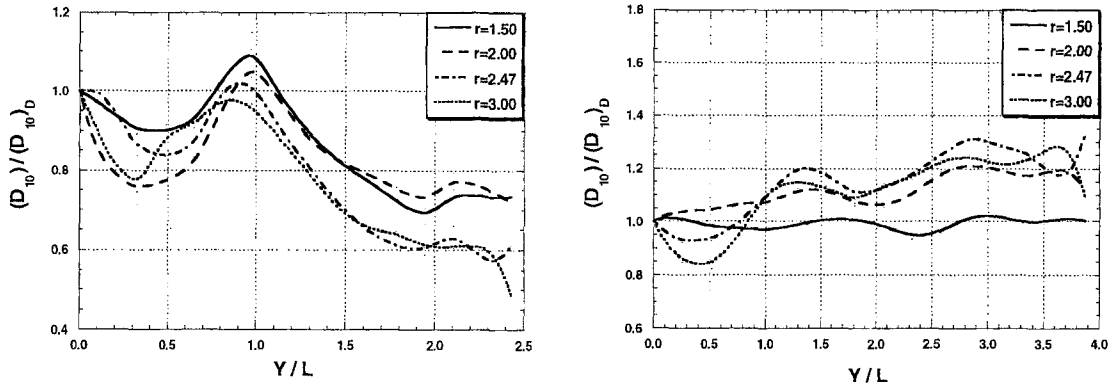

(a) $Z=30$mm (b) $Z=100$mm

Fig. 7 $D_{10}/(D_{10})_D$ distribution along the centerline ($X=0$mm) for No. 1 injector

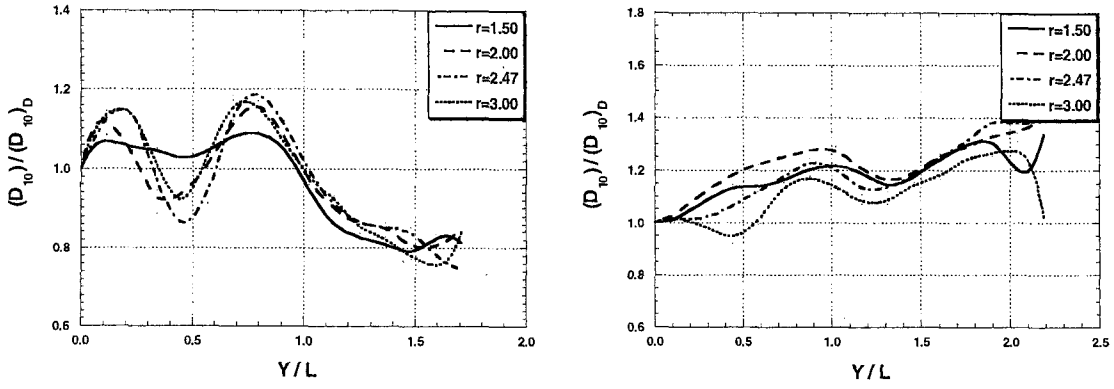

(a) $Z=50$mm (b) $Z=100$mm

Fig. 8 $D_{10}/(D_{10})_D$ distribution along the centerline ($X=0$mm) for No. 3 injector

sionalized with the $(D_{sdev})_D$ at X=0mm and Y=0mm for No. 1 and 2 injectors in Fig. 9 and 10. The standard deviation is similarly distributed to the SMD. The standard deviation of droplet size increases with the mixture ratio. This is because the disintegrated length from liquid sheet into droplets becomes longer with increasing the mixture ratio, so that the droplet size becomes non-uniform. As shown in Fig. 9, the standard deviation of droplet size becomes smaller in the interaction area irrespective of the mixture ratio. The reason for the small D_{sdev} value in the interaction area similarly to the SMD and arithmetic mean diameter of droplets is because the droplet size becomes uniform, which small droplets become larger due to the coalescence and large droplets become smaller due to the disintegration as droplets impinge each other in the interaction area. In case of the No. 2 injector in Fig. 10, the $D_{sdev}/(D_{sdev})_D$ distribution in the interaction area is similar to that for No. 1 injector.

3.2 Axial velocity

Figure 11 indicates the axial velocity distribution in the X-Y plane at r=2.0 and 3.0 for No. 1. The axial velocity reaches the highest value in the center of the single spray just after starting injection. Then, sprays from two single sprays superpose with moving into the downstream region, so that one uniform velocity region is formed between Z=75mm and Z=100mm. This is because the momentum loss by disintegration of droplets causes the decrease of velocity. As the mixture ratio increases, fuel jets have a difficulty to break up oxidizer jets. Therefore, the effect of

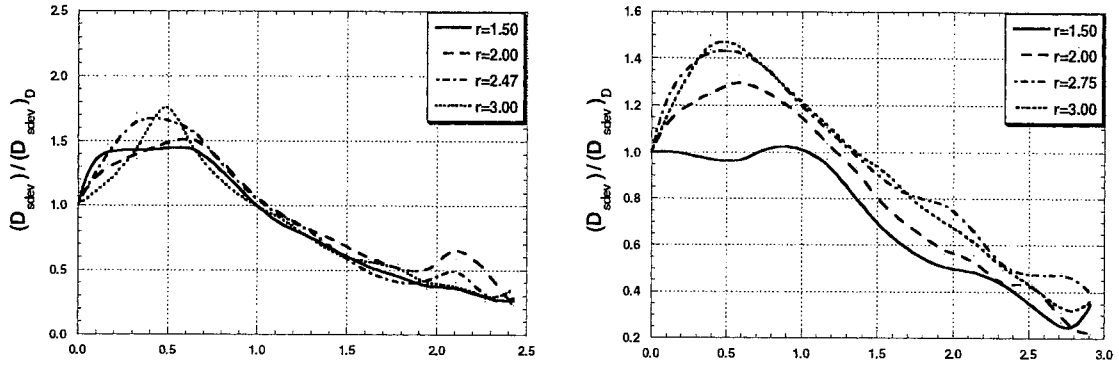

(a) Z=30mm (b) Z=50mm

Fig. 9 $D_{sdev}/(D_{sdev})_D$ distribution along the centerline (X=0mm) for No. 1 injector

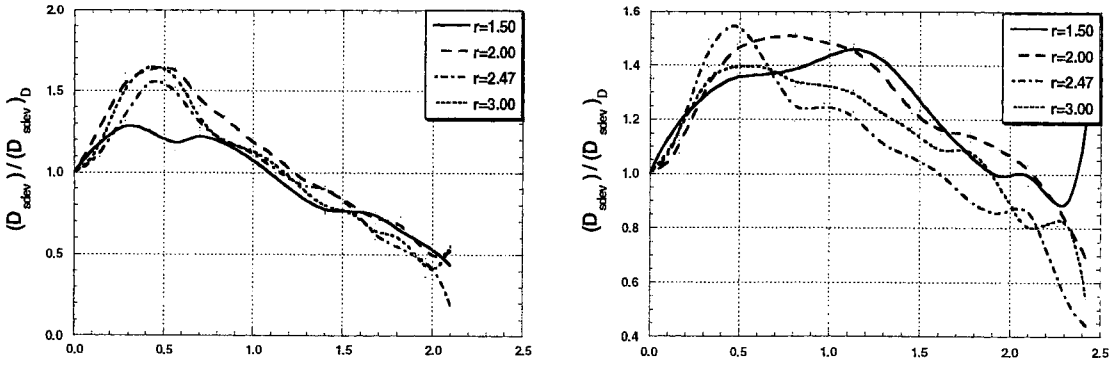

(a) Z=30mm (b) Z=75mm

Fig. 10 $D_{sdev}/(D_{sdev})_D$ distribution along the centerline (X=0mm) for No. 2 injector (L=31.2mm)

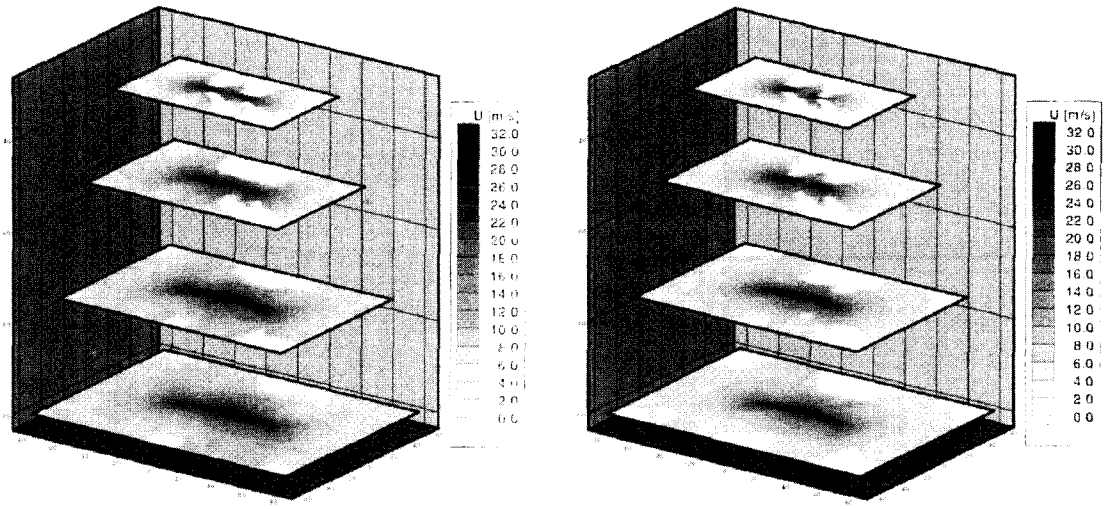

(a) $r=2.00$ (b) $r=3.00$

Fig. 11 Axial velocity distribution for No. 1 injector ($L=20.8$mm)

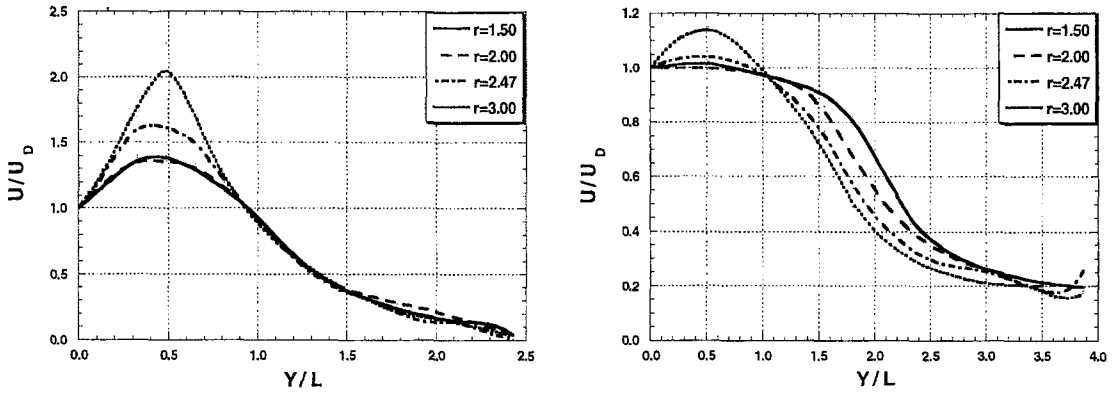

(a) $Z=30$mm (b) $Z=100$mm

Fig. 12 U/U_D distribution along the centerline ($X=0$mm) for No. 1 injector

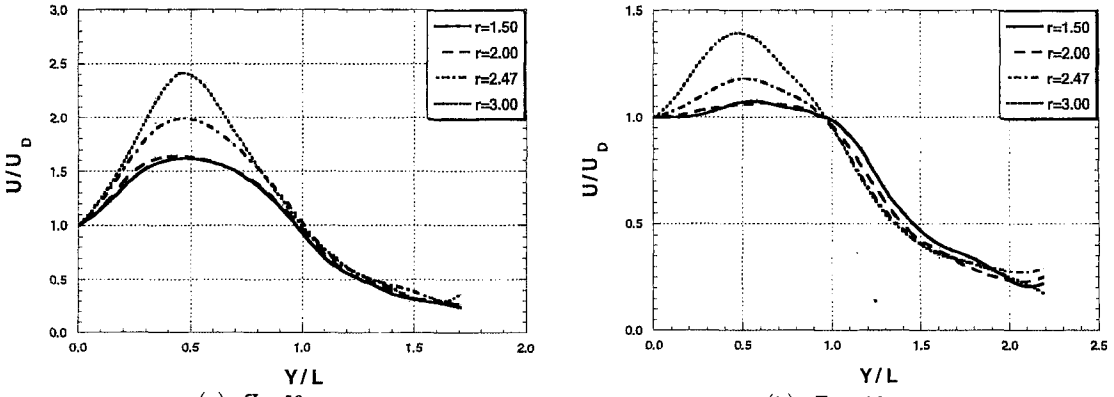

(a) $Z=50$mm (b) $Z=100$mm

Fig. 13 U/U_D distribution along the centerline ($X=0$mm) for No. 3 injector

oxidizer jets which have strong momentum is exerted to $Z=100$mm where the axial velocity is considerably high.

In Fig. 12 and 13, the axial velocity (U) measured in the center, $X=0$mm, along the Y direction is non-dimensionalized with U_D at $X=0$mm and $Y=0$mm for No. 1 and 3 injectors. The U/U_D value at $Z=30$ and 100mm is slightly smaller than 1 in $Y/L=1$. This is because droplets disintegrated from the right side injector have a different Y-direction velocity from those disintegrated from the left side injector but have a same axial velocity as. Consequently, the Y-direction velocity is offset but the axial velocity increases more after the impingement in the interaction area. This tendency is typical regardless of the injector interval. The increase of the axial velocity in the interaction area is less than 7% of U_D.

3.3 *We* number

Arkhipov et al. (1982) and Pazhi et al. (1976) suggested the disintegration mechanism after the impingement between droplets. Arkhipov et al. (1982) investigated the effect of the angular momentum and *We* number on the disintegration. They insisted that the possibility to disintegrate into small droplets goes up with increasing the angular momentum and with increasing the relative velocity of impinged droplets. Pazhi et al. (1976) studied the *We* number by the relative velocity difference of impinged droplets. They suggested that if the relative velocity of impinged droplets is low, the possibility to become larger droplets by coalescence goes up, but droplets can be disintegrated by the aerodynamic disturbance at this time. However, if the relative velocity is high, droplets instantaneously coalesce just after impingement, and then those disintegrate again into small droplets which have a similar size before impingement or have a lot of smaller size droplets. Hence, the *We* number is analyzed in order to investigate the background of the decrease of the SMD, arithmetic mean diameter and standard deviation of droplets in the interaction area.

The PDPA system cannot measure Weber number by the angular momentum and relative velocity difference, since it cannot distinguish the velocity and size of two impinged droplets. However, Weber number of droplets in the interaction area can be calculated. The axial and radial velocities were measured at various points by using the PDPA system. There are two assumptions to calculate Weber number.

First, the case of impingement of two droplets that have the same size and velocity is concerned. Two sprays from two F-O-O-F injectors can be regarded as the same, so that it can be assumed that droplets in $Y=+L$mm are the same as those

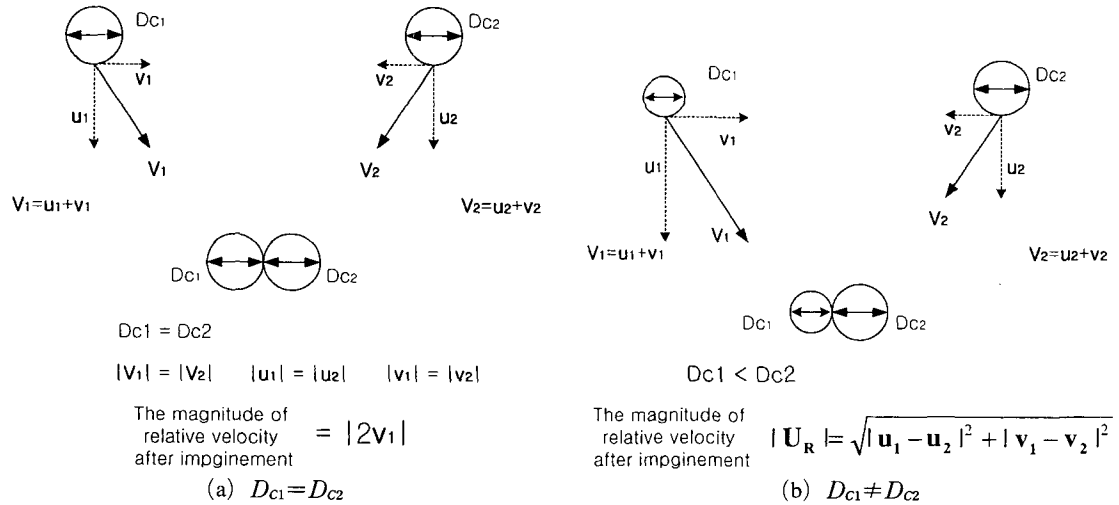

Fig. 14 Schematic drawing of model of drop collision

in $Y=-L$mm. Droplets in $Y=\pm L$mm can be regarded as droplets toward the centerline, $Y=$ 0mm, and colliding each other. Since two colliding drops have the same size and velocity, the axial velocity component is offset and the radial velocity increases twice after impingement, as shown in Fig. 14(a). Weber number calculated in this case is defined as Eq. (2).

$$We=\frac{\rho_L |2\boldsymbol{v}|^2 (D_{10})_C}{\sigma_L} \tag{2}$$

Where $\boldsymbol{v}$ is the radial velocity component and $(D_{10})_C$ is the arithmetic mean diameter. Since impinged droplets are not influenced by the density of surrounding air but by the momentum of impinged droplets, the density of the droplet is used to calculate.

Figure 15 indicates the $(D_{10})_D/(D_{10})_C$ distribution for Weber number. The $(D_{10})_D/(D_{10})_C$ value over 1 means droplets are coalesced by impingement in the cross region, and the divided value below 1 means droplets are disintegrated by impingement. The $(D_{10})_D/(D_{10})_C$ value exceeds 1 only for low Weber number below 40, which means the possibility to coalesce goes up after interaction. On the other hand, if Weber number of colliding droplets exceeds 40, the possibility to disintegrate into small droplets goes up in the interaction area. The divided value is getting smaller with increasing Weber number. The empirical equation of the size change of drops which impinge with high momentum can be obtained by the curve fitting of these data. The empirical equation is given by

$$\frac{(D_{10})_D}{(D_{10})_C}=1.1997-0.19342\log(We) \tag{3}$$

Second, the case of impingement of two droplets that have the different size and velocity is concerned. Droplets existed in $Y=+L$mm should have the same properties as those in $Y=-L$mm theoretically, but have the different size and velocity in practice. If droplets are existed in the same X and Z plane, it is regarded that those in $Y=+L$mm and $Y=-L$mm are impinged in the interaction area, as shown in Fig. 14(b). Therefore, Weber number is obtained by using the relative velocity of two droplets existed in $Y=+L$mm and $Y=-L$mm, and the arithmetic mean diameter of small droplet between two. Weber number calculated in this case is defined as Eq. (4).

$$We=\frac{\rho_L U_R^2 (D_{10})_{small}}{\sigma_L} \tag{4}$$

Where U_R is the relative velocity between droplets and $(D_{10})_{small}$ is the arithmetic mean diameter of small one between two colliding droplets.

Figure 16 indicates the $(D_{10})_D/(D_{10})_{small}$ distribution for Weber number. The distribution trend is similar to the first case, but the gradient for high Weber number is gentler because colliding droplets have different size and velocity so that droplets are disintegrated into various sizes after impingement. The empirical equation for the second case is given by

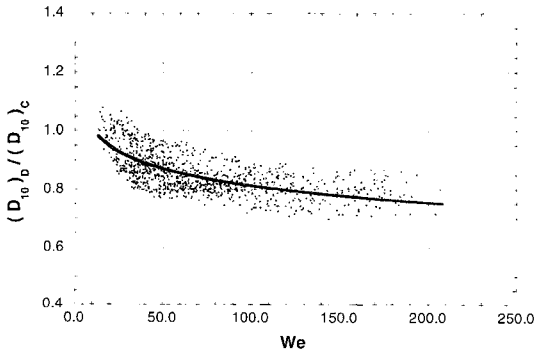

Fig. 15 $(D_{10})_D/(D_{10})_C$ distribution along Weber number ($D_{C1}=D_{C2}$)

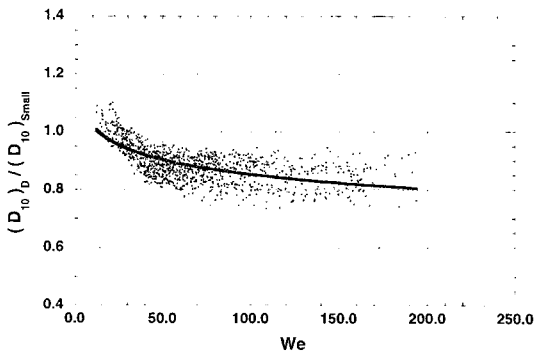

Fig. 16 $(D_{10})_D/(D_{10})_{small}$ distribution along Weber number ($D_{C1}\neq D_{C2}$)

$$\frac{(D_{10})_D}{(D_{10})_{small}} = 1.1887 - 0.16754 \log(We) \quad (5)$$

Acknowledgement

This work was supported by the grant of Post-Doc. Program, Chonbuk National University (2000).

Conclusion

Through the PDPA analysis of twin spray characteristics of two impinging F-O-O-F type injectors in the interaction area concluding remarks can be summarized as following.

(1) Comparing the SMD (D_{32}), arithmetic mean diameter (D_{10}) and standard deviation (D_{sdev}) of droplets in line D with those in line C in Fig. 1(b), those were 6~20% smaller in the interaction area (line D). Consequently, it is concluded that droplets become uniform and disintegrate into smaller ones after impingement in the interaction area.

(2) The axial velocity of droplets in the interaction area, line D, was 5~7% higher than those in line C, since the direction of axial velocity of droplets disintegrated from the right side injector is same as those from the left side injector. But that of Y-direction velocity is different.

(3) For the $(D_{10})_D/(D_{10})_C$ value, an empirical Correlation is obtained under the assumption of two identical impinging droplets as

$$\frac{(D_{10})_D}{(D_{10})_C} = 1.1997 - 0.19342 \log(We)$$

An empirical correlation is obtained for the $(D_{10})_D/(D_{10})_{small}$ value under the assumption that a droplet is impinged by one with different size and velocity as

$$\frac{(D_{10})_D}{(D_{10})_{small}} = 1.1887 - 0,\ 16754 \log(We)$$

Droplets with low Weber numbers below 40 tend to coalesce, while those over 40 tend to disintegrate after impingement.

References

Arkhipov, V. A., Bushlanov, V. P., Vasenin, I. M., Rusakov, V. V. and Trokhimov, V. F., 1982, "Equilibrium Forms and Stability of Rotating Drops," *Mekh. Zhidkosti I gaza*, No. 4.

Kang, S. J., Rho, B. J., Oh, J. H. and Kwon, K. C., 2000, "Atomization Characteristics of a Double Impinging F-O-O-F type Injector with Four Streams for Liquid Rocket," *KSME International Journal*, Vol. 14, No. 4, pp. 466~476.

Kang, S. J., Ryu, K. W., Kwon, K. C. and Song, B. K., 2001, "An Experimental Study on Turbulent Characteristics of an Impinging Split-Triplet Injector," *KSME International Journal*, Vol. 15, No. 1, pp. 117~124.

Kuykendal, W. B., 1970, "The Effects of Injector Design Variables on Average Drop Size for Impinging Jets," AFRPL-TR-70-53.

Park, S. Y., Kim, S. J., Park, S. U. and Kim, Y., 1996, "A Study on Atomization Characteristics of an Impinging Triplet Injector," *Transactions of KSME*, Vol. 20, No. 3, pp. 1005~1014.

Pazhi, D. L. and Galustov, V. S., 1976, "Liquid Atomizers," Khimiya, Moscow.

Rupe, J. H., 1956, "A Correlation Between the Dynamic Properties of a Pair Impinging Streams and the Uniformity of Mixture Ratio Distribution in the Resulting Spray," *Jet Propulsion Laboratory, California Institute of Technology*, Pasadena, California.

Yoon, S. J., Cho, D. J., 1992, "A Study on the Spray characteristics due to Droplet Collision in Cross Region of Twin Spray System," *KSME 1992 Fall Annual Meeting* (II), pp. 276~280.